

# UC Davis

## UC Davis Previously Published Works

### Title

Make It a Double? Sobering Results from Simulations Using Single-Moment Microphysics Schemes

### Permalink

<https://escholarship.org/uc/item/39x70334>

### Journal

Journal of the Atmospheric Sciences, 72(2)

### ISSN

0022-4928

### Authors

Igel, Adele L  
Igel, Matthew R  
van den Heever, Susan C

### Publication Date

2015-02-01

### DOI

10.1175/jas-d-14-0107.1

Peer reviewed

## Make It a Double? Sobering Results from Simulations Using Single-Moment Microphysics Schemes

ADELE L. IGEL, MATTHEW R. IGEL, AND SUSAN C. VAN DEN HEEVER

*Department of Atmospheric Science, Colorado State University, Fort Collins, Colorado*

(Manuscript received 16 April 2014, in final form 24 October 2014)

### ABSTRACT

Single-moment microphysics schemes have long enjoyed popularity for their simplicity and efficiency. However, in this article it is argued through theoretical considerations, idealized thunderstorm simulations, and radiative–convective equilibrium (RCE) simulations that the assumptions inherent in these parameterizations can induce large errors in the proper representation of clouds and their feedbacks to the atmosphere. For example, precipitation is shown to increase by 200% through changes to fixed parameters in a single-moment scheme and low-cloud fraction in the RCE simulations drops from about 15% in double-moment simulations to about 2% in single-moment simulations. This study adds to the large body of work that has shown that double-moment schemes generally outperform single-moment schemes. Therefore, it is recommended that future studies, regardless of their focus and especially those employing cloud-resolving models to simulate a realistic atmosphere, strongly consider moving to the exclusive use of multimoment microphysics schemes.

### 1. Introduction

The parameterization of cloud microphysics has long been one of the greatest challenges for atmospheric models with grid spacings of a few kilometers or less. Because of the small length scale at which microphysical processes occur (microns to millimeters) and the sheer number of cloud droplets, ice crystals, and raindrops (up to about  $10\,000\text{ cm}^{-3}$ ), it is not feasible to simulate microphysical processes explicitly in domains with volumes of even a few cubic kilometers given current computational resources. Many microphysical parameterization frameworks, wherein microphysical processes are not explicitly simulated, have therefore been designed to circumvent this problem—the two most frequently used today being single-moment and double-moment bulk schemes.

The goal of this paper is to motivate the use of double-moment schemes over single-moment schemes. This will be done in several ways. First, here in the introduction, an overview of microphysics schemes is given, and the past work comparing single- and double-moment

schemes is presented. In [section 2](#), the sensitivity of different microphysical processes to fixed parameters that are necessary in single-moment schemes will be investigated from a simple theoretical perspective. In [section 3](#), idealized simulations of convection using a single-moment scheme are presented to show the range of results that can be achieved by simply changing the fixed parameters. Though the differences obtained in simulations using single- and double-moment schemes have been described in the past, less attention has been given to the range of results that can be achieved by varying the fixed parameters within the same single-moment scheme such as has been done by [Ferrier et al. \(1995\)](#), [Gilmore et al. \(2004\)](#), [van den Heever and Cotton \(2004\)](#), [Yussouf and Stensrud \(2012\)](#), and [Adams-Selin et al. \(2013\)](#). The range of results will be demonstrated for a simple simulation in this study to advocate further for the phasing out of single-moment schemes, particularly when conducting research simulations. Last, comparisons between simulations run with both single- and double-moment schemes for a system in radiative–convective equilibrium (RCE) are presented in [section 4](#). Basic comparisons are made between observations and the RCE simulations that suggest that the double-moment simulations capture the tropical cloud and precipitation characteristics more realistically than single-moment schemes.

---

*Corresponding author address:* Adele L. Igel, Department of Atmospheric Science, 1371 Campus Delivery, Fort Collins, CO 80523.  
E-mail: [adele.igel@colostate.edu](mailto:adele.igel@colostate.edu)

Single-moment schemes require minimal memory and computational burden compared to more complex schemes. Many single-moment schemes predict the mixing ratio of each hydrometeor species and keep either the mean diameter or number concentration fixed, such that the other can be diagnosed (Lin et al. 1983; Walko et al. 1995; Straka and Mansell 2005; Hong and Lim 2006). Depending on the complexity of the scheme, the size distribution of each species can be monodisperse, or a distribution shape may be assumed. In the case of an assumed exponential distribution, the intercept parameter is commonly held constant rather than the number concentration or the mean diameter. Irrespectively, there is a fixed relationship between number concentration, diameter, and other specified parameters of the assumed distribution. Though not common, some schemes diagnose the intercept parameter based on environmental conditions so that it can vary in space and time (Hong et al. 2004; Thompson et al. 2004). Nonetheless, the inability of single-moment schemes to allow the number concentration and mean diameter of hydrometeors to vary independently severely limits their ability to simulate clouds with characteristics consistent with observations across a wide range of atmospheric conditions.

Double-moment schemes, as their name implies, predict two moments of the distribution, usually the mixing ratio and number concentration of each hydrometeor species (Ferrier 1994; Meyers et al. 1997; Milbrandt and Yau 2005a; Morrison et al. 2005; Seifert and Beheng 2006; Mansell et al. 2010). Some schemes are mixed moment with one moment of some hydrometeor species being predicted, such as cloud water and ice crystals, and two moments of other species being predicted (Thompson et al. 2008; Hong et al. 2010). Double-moment schemes allow for a more realistic representation of clouds, since both number concentration and diameter are allowed to vary independently in space; however, the shape of the distributions usually remains fixed. A fixed distribution shape is not always the case; Milbrandt and Yau (2005a), for example, developed diagnostic equations for the shape parameter of the precipitating hydrometeors.

When both the mixing ratio and number concentration of a hydrometeor species are predicted, the representation of many microphysical processes can be improved. Two such processes—condensation and collision-coalescence—are discussed below in section 2. Another process that is improved is sedimentation, or the falling of hydrometeors (Wacker and Seifert 2001; Milbrandt and Yau 2005a; Milbrandt and McTaggart-Cowan 2010). In the real atmosphere, large, more massive drops fall faster than small drops, which leads to an

effect known as size sorting. Size sorting cannot be predicted in a single-moment scheme unless one of the fixed parameters is allowed to vary with height (Milbrandt and McTaggart-Cowan 2010) but can be predicted in any multimoment scheme by using different fall velocities for the different predicted moments of the hydrometeor size distribution. Though generally sedimentation is improved in double-moment schemes over single-moment schemes, double-moment schemes tend to be overly aggressive in their sorting, and methods have been suggested to ameliorate this problem (Milbrandt and Yau 2005a; Wacker and Lüpkes 2009; Mansell 2010; Milbrandt and McTaggart-Cowan 2010).

While the representation of microphysical processes can be improved since more variables exist in double-moment schemes than single-moment schemes to describe the cloud properties, new assumptions must also be made. For example, since the predicted mean diameter of rain can reach large values, the raindrop breakup process must be parameterized. However, this is a poorly understood process, and simulations can be sensitive to how it is implemented (Morrison and Milbrandt 2011; Morrison et al. 2012; Van Weverberg et al. 2014). Also, the number and size of raindrops to create during processes such as hail shedding and ice melting need to be parameterized, but they are not constrained well by observations (e.g., Meyers et al. 1997). Uncertainties exist regarding how many cloud droplets and ice crystals to create upon nucleation. Such decisions usually require some assumptions about the aerosol particle distribution. The Hallett–Mossop ice multiplication process is another poorly understood ice nucleation mechanism that can have large impacts on cloud properties depending on how it is parameterized (Connolly et al. 2006). These are just some of the problems that must be addressed in double-moment schemes but not in single-moment schemes.

Despite these new assumptions, double-moment schemes have been shown to be generally more successful than single-moment schemes in reproducing observations of a number of different cloud systems including squall lines (Morrison et al. 2009; Van Weverberg et al. 2012; Baba and Takahashi 2014), supercells (Dawson et al. 2010; Jung et al. 2012), scattered and isolated convection (Swann 1998), mesoscale cloud systems (Lee and Donner 2011), tropical cyclones (Jin et al. 2014), Arctic mixed-phase stratus clouds (Luo et al. 2008), orographic clouds (Milbrandt et al. 2010), Colorado winter storms (Reisner et al. 1998), and synoptic-scale snow events (though single-moment schemes with diagnosed intercept parameters did well) (Molthan and Colle 2012). These studies have shown improvements in the representation of a wide range of atmospheric variables

including liquid and ice water contents, precipitation, radiative fluxes, cold-pool properties, storm morphology, and dynamics with the use of double-moment schemes. Van Weverberg et al. (2014) found that the two kinds of schemes do equally well when simulating very intense precipitation owing to the poor representation of rain breakup in double-moment schemes. Relatively few studies have shown no improvement with the use of double-moment schemes (Van Weverberg et al. 2013; Wu and Petty 2010).

The improvement that is usually found in simulations when using double-moment schemes rather than single-moment schemes does come with increased computation time and memory requirements. That being said, computational capabilities have been rapidly increasing and it is suggested here that simulations run for research purposes should no longer use single-moment schemes. Regardless of whether the focus of a given study is on microphysical processes, the choice of microphysics scheme will influence the simulated outcome through a multitude of dynamic, radiative, thermodynamic, and microphysical feedback processes. Therefore, double-moment parameterizations should be chosen over single-moment parameterizations whenever possible in order to obtain better results as demonstrated by the studies cited above and as will be demonstrated below in the current study.

It should be noted that other kinds of microphysics parameterizations exist for cloud-resolving models but are less common. Triple-moment schemes (Milbrandt and Yau 2005b) predict the shape parameter of the gamma probability distribution using prognostic equations for the radar reflectivity, which is the sixth moment of the distribution. Spectral bin schemes (Reisin et al. 1996; Ovtchinnikov and Kogan 2000; Rasmussen et al. 2002; Khain et al. 2004; Lebo and Seinfeld 2011) avoid the need to assume a size distribution function by dividing the distribution of a species into discrete bins and prognosing the number and/or the mass mixing ratio of each bin separately. Uniquely, Onishi and Takahashi (2012) developed a scheme with a bin representation of the warm-phase species and a two-moment bulk representation of the ice-phase species. Bin-emulating schemes (Feingold et al. 1998; Saleeby and Cotton 2004, 2008; Saleeby and van den Heever 2013) have been designed to take advantage of both bulk and bin schemes—they are double-moment schemes that use lookup tables for some microphysical process rates that have been generated from bin schemes. Finally, the superdroplet method of parameterizing microphysics (Shima et al. 2009) uses a novel approach in which the position and physical properties of a collection of droplets with identical attributes (or a superdroplet) are

prognosed. To date, the parameterization has only been developed for the warm phase. These kinds of schemes can be good alternatives to single- and double-moment schemes depending on the application, although all of them are more computationally expensive.

## 2. Theoretical considerations

In this section, the sensitivity of microphysical processes to fixed hydrometeor distribution parameters is explored. For simplicity, the focus of the discussion in this section is on the representation of warm-phase microphysical processes in single-moment schemes—specifically, condensation and autoconversion. However, similar reasoning could just as easily be applied to the ice phase for deposition, riming, and other collection processes. Note that the processes discussed have more complex representations in most microphysical schemes than are described here. This section is only intended to provide a qualitative sense for the sensitivity of each process.

Condensation is the first process considered here. In some models, a saturation adjustment scheme is employed to calculate condensation. In such schemes, any supersaturation that develops is depleted immediately to form liquid water. When using saturation adjustment schemes, both single- and double-moment schemes will predict the same amount of condensation given the same supersaturation at any grid point. Lebo et al. (2012) have recently discussed saturation adjustment schemes in much more depth.

In other models, saturation adjustment is not implemented, in which case the condensation equation is represented explicitly in some form. This form will depend on the assumed size distribution of the hydrometeors. The gamma size distribution is commonly assumed such that the mixing ratio can be expressed as

$$r = \frac{N_T}{\rho_a} \frac{\pi}{6} \left( \frac{\bar{D}}{\nu} \right)^3 \frac{\Gamma(\nu + 3)}{\Gamma(\nu)} \quad (1)$$

(e.g., Walko et al. 1995), where  $N_T$  is the total number concentration of droplets,  $\bar{D}$  is the mean number diameter,  $\nu$  is the distribution shape parameter, and  $\rho_a$  is air density. If  $\nu = 1$ , then the distribution is equivalent to a Marshall–Palmer distribution. Following Walko et al. (1995) and neglecting the effects of ventilation, the equation for the rate of condensation  $C$  (the time rate of change of the hydrometeor mass mixing ratio) can be expressed simply as

$$C = \frac{\partial r}{\partial t} = 2\pi(S - 1)GN_T\bar{D}, \quad (2)$$

TABLE 1. Summary of the sensitivity of process rates to a fixed mean diameter and fixed number concentration of cloud droplets as described in section 2.

Change in the process rate when ...	Condensation/evaporation	Collision-coalescence
Diameter is doubled	$\div 4$	$\times 2$
Number concentration is doubled	$\times 1.6$	$\div 1.3$
Number concentration is increased tenfold	$\times 4.6$	$\div 2.2$

where  $S$  is the saturation ratio and  $G$  is a function of temperature and pressure that represents the impacts of latent heat release and other nonlinearities, the specifics of which are not germane to the discussion.

These equations can be used to show how the properties of a distribution will impact condensation rates in a single-moment scheme. It can be seen from Eq. (1) that for a fixed mixing ratio and a fixed shape parameter  $N_T \propto \bar{D}^{-3}$ . By substituting this relationship into Eq. (2) it can be shown that  $C \propto \bar{D}^{-2}$  for a fixed diameter or that  $C \propto N_T^{2/3}$  for a fixed number concentration, all else being equal. The different powers on diameter and number concentration in these simple relationships indicate that the condensation rate will be comparatively more sensitive to the choice of fixed diameter. For example, for a doubling in the choice of fixed diameter, the condensation rate will be reduced by a factor of 4. On the other hand, a doubling of the fixed number concentration will increase condensation by only a factor of 1.6. Thus, changing either parameter will result in significant changes to the condensation rate, with the rate being more sensitive to changes in mean diameter. While such variability of the diameter and number concentration is common in real-world clouds, it cannot be represented by single-moment schemes. It should be noted though that when the supersaturation is low enough to be almost entirely consumed in one time step, saturation adjustment and supersaturation allowing condensation schemes will give very similar answers and the sensitivity to fixed parameters will be reduced.

The sensitivity of collision-coalescence to the choice of the fixed parameter in single-moment schemes is more difficult to determine because there are many different ways in which this process has been parameterized. Sophisticated Kessler-type parameterizations (e.g., Manton and Cotton 1977; Baker 1993; Boucher et al. 1995; Liu and Daum 2004) show the autoconversion rate to be proportional to  $N_T^{-1/3}$  with no dependence on  $\bar{D}$ . Given that  $N_T \propto \bar{D}^{-3}$ , the autoconversion rate must be proportional to  $\bar{D}$  if the diameter is fixed. Using the same example as before, doubling a fixed diameter will double the autoconversion rate, and doubling a fixed number concentration will decrease the rate by a factor of 1.3 and by a factor of 2.2 for a tenfold increase. As with the condensation rate, we see that the autoconversion

rate is more sensitive to a change in the mean diameter than to a change in the number concentration.

As shown above and summarized in Table 1, condensation and collision-coalescence have sensitivities to  $N_T$  and  $\bar{D}$ , although in the opposite sense. That is, growth of cloud water through condensation is increased and depletion through collision-coalescence is decreased for either a decrease in mean diameter or an increase in number concentration, assuming the same cloud water content. Therefore, the two processes will feed back on one another to cause cloud water content to be even more disparate for a change in diameter or number concentration. For example, during a single model time step for a fixed cloud water content, a population of larger, less numerous cloud droplets ( $\bar{D} \uparrow, N_T \downarrow$ ) will grow more slowly and have less additional mass at the end of the time step than a population of smaller, more numerous droplets ( $\bar{D} \downarrow, N_T \uparrow$ ). During the same time step, this population of droplets ( $\bar{D} \uparrow, N_T \downarrow$ ) will self-collect more quickly to create rain, further reducing the cloud water content relative to the scenario with smaller, more numerous droplets ( $\bar{D} \downarrow, N_T \uparrow$ ). The processes act together to reduce the amount of cloud water present at the next model time step in ( $\bar{D} \uparrow, N_T \downarrow$ ) relative to ( $\bar{D} \downarrow, N_T \uparrow$ ). These processes and their subsequent feedbacks occur simply because of somewhat arbitrarily chosen microphysical parameters. Owing to the nonlinear interaction of these processes as well as their different time scales, it is difficult to determine a priori how much quantities such as cloud water mixing ratio will vary because of changes in the fixed parameter values. The full implications of these changes in condensation and collision-coalescence rates and all other process rates, especially when multiple liquid and ice hydrometeors are being simulated, are best explored by running numerical simulations.

### 3. Simulations with single-moment schemes

#### a. Simulation design

To explore the range of results that can be obtained by simply changing the value of a fixed parameter, simulations of an idealized ordinary thunderstorm are run using the Regional Atmospheric Modeling System (RAMS) (Cotton et al. 2003). RAMS is used because its

TABLE 2. Summary of the microphysical parameters used in the idealized thunderstorm and RCE simulations. The parameter that is fixed is indicated with a “D” for mean diameter, “N” for number concentration, or “P” if it is predicted (i.e., the double-moment scheme is being used). The unit for the cloud diameter is micrometers; all other diameters are given in millimeters. The number concentration is given in number per milligram and is italicized as a reminder that it is not a diameter. Note that the aerosol number concentration is a prognostic variable and that the value given is the initial concentration at the surface. Values that are not the default values are boldface. Values for SM\_AVG are the mass-weighted average values for the restart time in DM\_A100. See the text for further details.

	Cloud	$N_{\text{drizzle}}$	$D_{\text{rain}}$	$D_{\text{snow}}$	$D_{\text{aggr}}$	$D_{\text{graupel}}$	$D_{\text{hail}}$	$N_{\text{aerosol}}$
Idealized thunderstorm simulations								
D5	<b>D – 5</b>	<i>0.1</i>	1	1	1	1	3	—
D25	<b>D – 25</b>	<i>0.1</i>	1	1	1	1	3	—
N100	<b>N – 100</b>	<i>0.1</i>	1	1	1	1	3	—
N1000	<b>N – 1000</b>	<i>0.1</i>	1	1	1	1	3	—
D25_RD0.3	<b>D – 25</b>	<i>0.1</i>	<b>0.3</b>	1	1	1	3	—
RCE simulations								
SM_DEF	<i>N – 300</i>	<i>0.1</i>	1	1	1	1	3	—
SM_AVG	<b>N – 40</b>	<b>0.2</b>	<b>0.2</b>	<b>0.3</b>	<b>0.9</b>	<b>0.7</b>	<b>1</b>	—
DM_A100	P	P	P	P	P	P	P	100
DM_A1000	P	P	P	P	P	P	P	1000

double-moment microphysics scheme (Meyers et al. 1997) can be run in a single-moment mode with either a fixed diameter or fixed number concentration. This capability allows for the exploration of the sensitivities of a simulation to either parameter. Many of the more recent advances to the RAMS double-moment scheme, such as its bin-emulating features and the second cloud mode (Saleeby and Cotton 2004, 2008; Saleeby and van den Heever 2013), were not used in order to keep the physics between the two schemes as similar as possible.

Four simulations of the idealized ordinary thunderstorm are performed: two with a fixed mean cloud droplet diameter and two with a fixed cloud droplet number concentration. The other species (rain, snow, aggregates, graupel, and hail) each have a fixed mean diameter and thus are also run in single-moment mode. The settings for the fixed parameters in each simulation are summarized in Table 2. Pristine ice is run in double-moment mode in all simulations since the single-moment option has been deprecated in RAMS. All species have a fixed distribution shape parameter of 2. Though only the cloud droplet properties are being varied in these experiments, it is expected that there will be changes to both the warm and ice phases of the storm as a result since ice is often nucleated from and can grow through the collection of supercooled cloud droplets. Both phases will therefore be examined here.

The values chosen for the fixed cloud droplet parameters in these sensitivity tests are meant to be representative of lower and upper limits of values typically used in previous studies. However, determining these limits is sometimes difficult as these values are frequently not reported in the literature. For the mean cloud droplet diameter, 5 and 25  $\mu\text{m}$  are chosen (referred to as D5 and D25, respectively), and for number

concentration, 100 and 1000  $\text{mg}^{-1}$  are selected (referred to as N100 and N1000, respectively). These values represent a reasonable range for the parameters based on observations (Pruppacher and Klett 2010, 10–30).

To simulate an isolated, deep convective storm, the convective sounding of Weisman and Klemp (1982) is used to initialize the domain homogeneously horizontally. The horizontal wind is set to zero to simulate an ordinary thunderstorm rather than a supercell. The model domain is  $200 \times 200 \text{ km}^2$  in area with a 1-km horizontal grid spacing. We use 40 levels in the vertical dimension with a grid spacing of 100 m at the surface being stretched to 1000 m aloft with the model top at 23.3 km. The model time step was 5 s. A 2-K warm, square bubble,  $20 \times 20 \text{ km}^2$  and 3 km deep, was used to initiate the convection.

### b. Cloud processes

Time series of cloud water growth (net condensation) and loss (autoconversion, accretion, riming) processes are shown in Fig. 1a along with the domain-average cloud water path (Fig. 1b). From these figures, it is clear that changing the cloud droplet properties has an immediate impact on the condensation and collision-coalescence rates that lead to changes in the total cloud water content. As expected from the theory discussed above in section 2, a smaller cloud droplet diameter (D5) leads to initially higher condensation rates and lower collision-coalescence rates, resulting in a cloud water path that is about 6 times larger than that for D25. Also as expected, N1000 initially has a condensation rate about 3% higher than N100, though the absolute difference is small and cannot be seen in Fig. 1a (N100, N1000). The collision-coalescence rate in N100 initially increases relative to N1000 as predicted by the theory

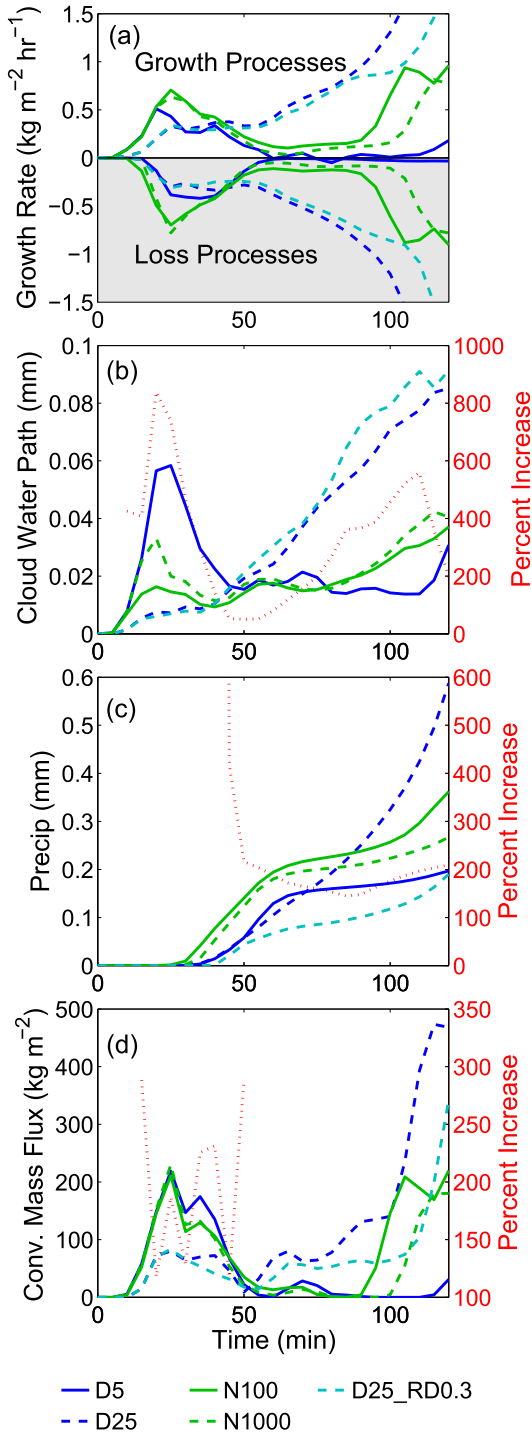


FIG. 1. Time series of domain-mean quantities. (a) Vertically integrated net condensation rate and loss rate of cloud water through autoconversion, accretion, and riming; (b) cloud water path; (c) accumulated precipitation; and (d) vertically integrated convective mass flux (see text for details). The red dotted lines in (b)–(d) correspond to the right axes and show the percentage increase of the maximum value among all five simulations relative to the minimum value among all five simulations as a function of time.

presented in section 2. Overall, these changes in process rates result in the cloud water path being highest for D5 and lowest for D25 and cause the initial trends in precipitation (Fig. 1c) to follow those of collision–coalescence.

For the most part, the initial changes in process rates are half as large or less than were predicted by theory (see section 2), probably because the assumption of fixed cloud water content is no longer valid. For example, while for the same cloud water content fewer but larger cloud droplets will collect more quickly to form rain and lead to less cloud water at the next time step, having less cloud water at the next time step will slow the collision–coalescence process. Therefore, because the cloud water content is now different, the difference in rate between the two scenarios will be less at the next time step than it was at the first time step.

The trends in convective mass flux (Fig. 1d), defined as the mass flux at points with vertical velocity greater than 1 m s<sup>-1</sup>, are in keeping with those for the condensation rate. Simulation D5 has a convective mass flux more similar to the constant number concentration cases, in part because so much of its cloud water is lofted above the freezing level where it causes increases in ice production and latent heating in the mixed-phase region (not shown). Simulation D25 has about 1/2 as much convective mass flux as the other three simulations during the first 40 min. The mass flux, and presumably the updraft speed, is reduced in D25 because of the relatively low condensational latent heating (Fig. 1a) and therefore reduced buoyancy. These changes in convective mass flux alter the morphology of the cloud and have implications for the subsequent development of the simulated storm.

After the initial 30–40 min, the microphysical feedbacks to the dynamics begin to dominate the differences between the simulations. It is emphasized that the purpose of this study is not to determine the pathways for these feedbacks but, rather, only to demonstrate that they exist and that they lead to uncertainties in the simulation results. The D25 case, though it had the least convective mass flux initially, sustains the mass flux during the middle period of the simulation and ultimately produces the most mass flux at the end of the simulation when secondary convection begins to develop. This fundamental change in the evolution of convection is reflected in the precipitation, cloud mixing ratio, and cloud process fields (Figs. 1a–c). The other three simulations appear to plateau to some degree in these fields whereas D25 continues to increase steadily. Ultimately, D25 produces greater than or in excess of 3 times more precipitation than its D5 counterpart. This is a significant increase considering that the only

difference in the setup of the two simulations is the mean size of the cloud droplets.

The sensitivity of these simulations to raindrop size is also briefly explored. The initial four simulations all had a fixed mean raindrop size of 1 mm. Based on a double-moment simulation of this same storm (not shown), 1 mm is a representative mean diameter for raindrops near the surface, but it is large for raindrops in rain formation regions. A fifth simulation (D25\_RD0.3) again uses a fixed cloud droplet size of  $25\ \mu\text{m}$  but reduces the mean raindrop diameter to 0.3 mm. In terms of cloud process rates, cloud water path, and convective mass flux, D25 and D25\_RD0.3 are more similar to each other than to any other simulation (Figs. 1a, 1b, and 1d). Nonetheless, convective mass flux during the second half of the two simulations becomes increasingly different, and the final precipitation produced in D25\_RD0.3 is significantly reduced (Fig. 1c), in part because of greater rain evaporation caused by small raindrops that evaporate more readily (not shown).

### c. Other thermodynamic and radiative impacts

The atmosphere is a complex system and, not surprisingly, these changes in cloud properties and dynamics impact many other aspects of this system. Changes to the precipitation amount and evaporation rates below cloud base lead to an average reduction in surface temperature of about 0.5 K between the warmest (D5) and coolest (D25\_RD0.3) simulations within the cold pool, where the cold pool is defined as all surface points with temperature less than the base-state surface temperature. In terms of forecasting daily temperature this may not be important, but it could be very important for cold-pool dynamics and subsequent convective development (Tompkins 2001). A number of other studies have also shown sensitivity of the cold-pool strength to choices in microphysical parameters (e.g., van den Heever and Cotton 2004; Dawson et al. 2010; Adams-Selin et al. 2013).

Upper-level tropospheric moisture is important as a chemical catalyst in the stratosphere and in its own right as a greenhouse gas. Figure 2b shows that up to 75% more moisture is available in the lower stratosphere in the D5 case, likely because more cloud water was available to be transported to the upper atmosphere to form ice in the anvil that subsequently sublimated. Accurately predicting stratospheric moisture has been shown to be critical to predicting long-term temperature trends of the lower stratosphere (Thompson et al. 2012).

Radiation is another factor that is impacted by changes to the single-moment scheme design. Differences in radiation will be largely driven by changes in cloud area, though total water content, hydrometeor

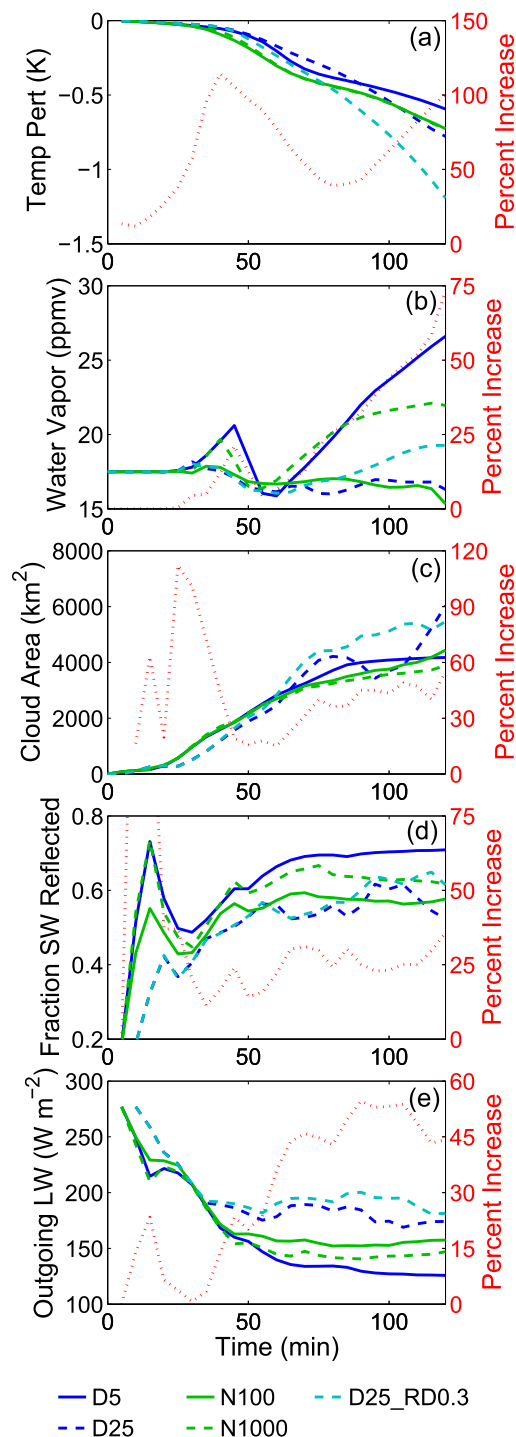


FIG. 2. Time series of (a) average cold-pool surface temperature perturbation relative to the initial environmental temperature, (b) water vapor mixing ratio averaged over a  $10000\text{-km}^2$  area centered around the storm at the first model level above the tropopause ( $13.3\text{ km}$ ), (c) cloud area, (d) fraction of incoming shortwave radiation reflected in cloudy columns, and (e) top-of-atmosphere outgoing longwave radiation in cloudy columns. A cloudy column in (c)–(e) is defined as a column with condensate mixing ratio at any level greater than  $0.01\text{ g kg}^{-1}$ . Red dotted lines are as in Fig. 1.



phase, and other hydrometeor properties will also play a role. Cloud area, reflected shortwave fraction, and outgoing longwave radiation are shown in Figs. 2c–e. A column is defined to be cloudy if one or more grid boxes have a hydrometeor mixing ratio greater than  $0.01 \text{ g kg}^{-1}$ . The radiative quantities have been averaged over cloudy columns; therefore, differences in these quantities between simulations do not account for changes in cloud area. The reflected shortwave radiation is consistently about 25% higher in D5 compared to D25 and N100 throughout the latter half of the simulations (Fig. 2c) owing to smaller cloud and ice particles. In terms of outgoing longwave radiation, the anvil in D25\_RD0.3 emits about 45% more longwave radiation than D5 (Fig. 2d), which is in part due to D25\_RD0.3 having a lower cloud-top height (not shown). These changes in radiation have implications for the radiative balance of the earth as simulated by cloud-resolving models (particularly when they are used for radiative–convective equilibrium simulations) and by GCMs and present yet another reason why moving away from single-moment schemes to double-moment schemes should be considered. To put one of these values in context, the 45% increase in emitted longwave radiation in D25\_RD0.3 compared to D5 would be on par with the magnitude of the largest deep convective cloud–climate feedback predicted by climate models (Zelinka and Hartmann 2010).

#### 4. Single- versus double-moment schemes

##### a. Simulation design

It could be argued that perhaps the simulations discussed in the previous section would not show such large differences if they were run for a longer period or over a larger domain. Furthermore, perhaps a similar range in sensitivity could be obtained by varying the aerosol concentration (which is arguably the primary control on the cloud droplet number concentration) in a double-moment simulation. To test some of these possibilities, results from large-domain and long-time RCE RAMS simulations are now presented.

These simulations were conducted at cloud-resolving grid scale (1 km) on a large domain ( $3000 \times 200$ ) with doubly periodic lateral boundary conditions and 65 vertical levels. The model top extends to 25-km altitude. This narrow grid setup has proven useful in the past to allow for large-scale flows while minimizing computational cost (Tompkins 2001; Posselt et al. 2008). The simulation is run for 70 days. The final 10 days will be used for analysis. As in van den Heever et al. (2011), the 0000 UTC 5 December 1992 tropical sounding from the

Tropical Ocean Global Atmosphere Coupled Ocean–Atmosphere Response Experiment (TOGA COARE) was used to initialize the temperature and moisture fields. Convection was induced with small, random perturbations to the potential temperature field. No mean wind was imposed, but a minimum wind speed of  $4 \text{ m s}^{-1}$  was used for the bulk surface flux calculations. A Smagorinsky (1963)–type turbulence scheme and the two-stream radiation scheme that is fully interactive with hydrometeors Harrington (1997) were used. These simulations are designed to represent the equilibrium state of the tropical atmosphere and contain the full range of tropical cloud types, from shallow, isolated cumulus through to large, deep convective complexes (van den Heever et al. 2011).

The base simulation is run with the double-moment scheme for 70 days; it is in RCE for approximately the latter half of that time. The base simulation is run with the double-moment microphysics scheme and has a horizontally and vertically homogeneous aerosol concentration of  $100 \text{ cm}^{-3}$ . This base simulation will be referred to as DM\_A100.

DM\_A100 is restarted on day 60 and run for 10 days with the single-moment microphysics scheme (SM\_DEF) rather than the double-moment scheme. The initial mixing ratio of all species is kept the same, but the number concentration and mean diameter all change instantaneously upon restart. This method of restarting DM\_A100 rather than starting a new simulation with the single-moment scheme and running it for 70 days is justified in the appendix. SM\_DEF is run with a fixed cloud droplet number concentration of  $300 \text{ mg}^{-1}$ . This droplet number concentration is the default value in RAMS; all other parameters are also run with the default values (see Table 2). While the default values may not be the most appropriate values to use, the default values may be a common and typical choice made by users of cloud models, especially those who are not experts in microphysics, regardless of the kind of simulation that they are running. Therefore, we want to explore the consequences of this potentially naïve choice in these RCE simulations.

A second sensitivity test has also been run in which an exponentially decreasing aerosol concentration profile is utilized (DM\_A1000). The profile maximizes at  $1000 \text{ cm}^{-3}$  at the surface and has a scale height of 2 km. The double-moment scheme is used for this test. It is presented to show a possible range of cloud characteristics for a change in aerosol concentration. Given that the increase in aerosol concentration in DM\_A1000 is relatively large, especially for the tropical maritime environment, we would hope that the differences in cloud properties arising through use of the single-moment

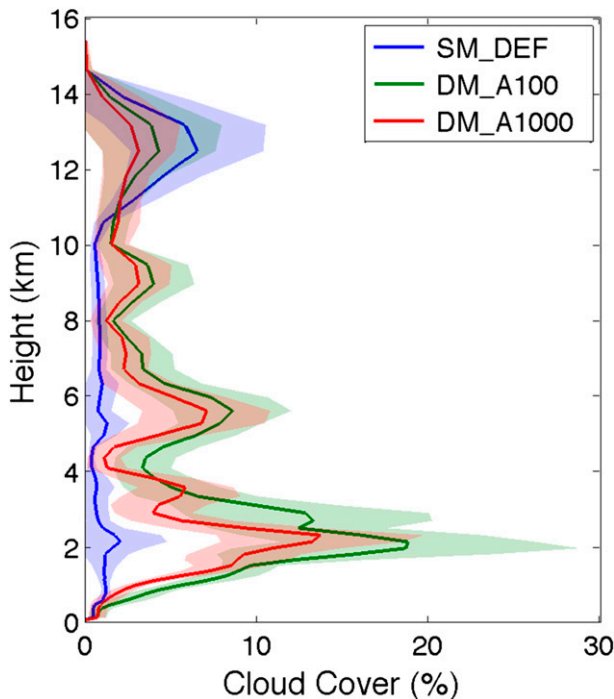


FIG. 3. Average cloud cover as a function of height in each of the three simulations. The shaded regions indicate one standard deviation in the time mean.

scheme would be no larger than those arising from this significant (and physically possible) increase in aerosol concentration.

#### b. Bulk cloud and rain properties

Average cloud fraction as a function of height from the three simulations is shown in Fig. 3 where the shading indicates one standard deviation in the time mean. At heights greater than 11 km, where anvil clouds associated with deep convection are present, the cloud fraction of the single-moment simulation is comparable to or exceeds those of the two double-moment simulations. Below 11 km, differences in the cloud fraction are larger. Peaks in cloud fraction at 5.5 and 9 km associated with congestus and detrainment at the freezing level (Johnson et al. 1999; Posselt et al. 2008) are reduced or not present in SM\_DEF. There is a peak around 2 km in all three simulations that indicates the shallow convective mode; however, in the single-moment simulation this peak is drastically reduced. It is approximately  $\frac{1}{6}$  the magnitude of the corresponding peak in cloud fraction for DM\_A100, and the shaded regions do not overlap. The tropical shallow cloud fraction as measured from *CloudSat* (Mace et al. 2009) and *CALIPSO* (Medeiros et al. 2010) is about 0.15–0.25, which indicates that the double-moment simulations capture the

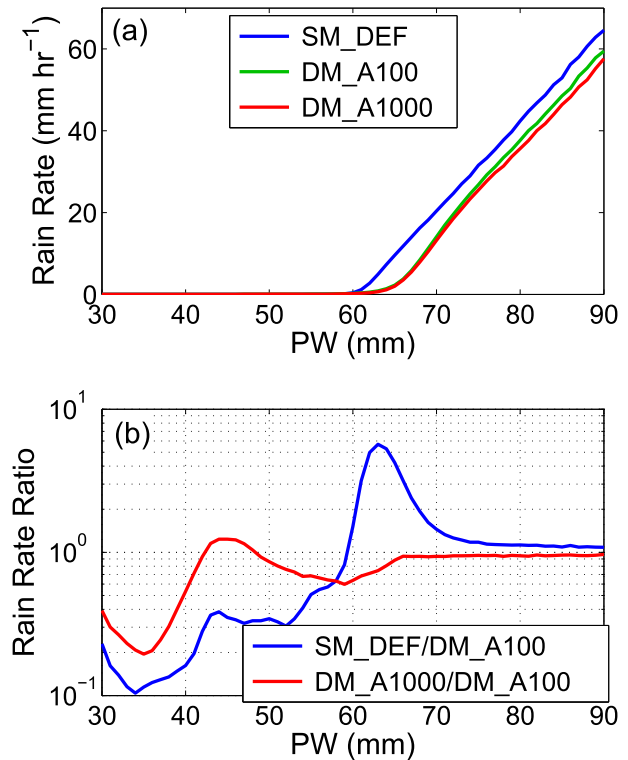


FIG. 4. (a) Average rain rate as a function of 1-mm precipitable water bins. (b) The ratio of the rain rates shown in (a) for selected pairs of the simulations.

frequency of these clouds more realistically. Additionally, although all of the RCE simulations underestimate the upper-level cloud fraction ( $\sim 12\%$ ; Mace et al. 2009), only the double-moment simulations correctly simulate more low-cloud fraction than high-cloud fraction.

Figure 4a shows the average rain rate as a function of precipitable water. The “critical” precipitable water (PW) value at which rain rates increase rapidly can be used to indicate the transition from shallow to deep convection and is a strong function of mean tropospheric temperature (Neelin et al. 2009). All of the RCE simulations have a mean tropospheric temperature of 273 K, which, based on observations, corresponds to a critical PW value of 68 mm (Neelin et al. 2009). For the two double-moment simulations, this value is about 65 mm, whereas for the single-moment simulation, it is about 60 mm. Again, the double-moment simulations agree more closely with the observations. The difference in these values can be put in context by noting that observations indicate that a decrease of 5 mm in this critical PW value occurs for a  $2^\circ\text{C}$  decrease in mean tropospheric temperature (Neelin et al. 2009)—a large value in the context of climate considerations. The mean temperature profiles among all the simulations, though, are very similar. This comparison suggests that the shift

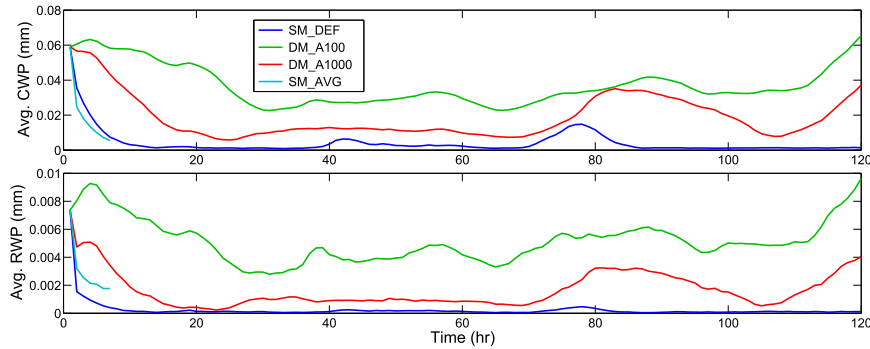


FIG. 5. Time evolution over the first 120 h of simulation of the average (top) cloud and (bottom) rainwater path (CWP, RWP) in low-PW regions ( $<40$  mm).

in the critical PW between the single- and double-moment simulations is large and could have important implications for the proper simulation of the tropical atmosphere.

Figure 4b shows the ratio of the mean rain rate as a function of PW for SM\_DEF and DM\_A1000 to that of DM\_A100. Associated with the reduction in cloud fraction for shallow convection in SM\_DEF is a 70%–90% reduction in the average rain rate for values of PW less than about 40 mm. This reduction in rain rate is consistently 10%–40% greater than that seen in DM\_A1000. Though much smaller, there is also a greater change in the convective rain rates (PW values greater than about 60–65 mm) in SM\_DEF than in DM\_A1000. These changes to the cloud fraction and rain rate of both deep and shallow convection are noteworthy since they are entirely driven by the differences in the microphysics scheme and because they are larger than changes that can be achieved by a tenfold increase in aerosol concentration in the double-moment scheme.

To investigate the cause of the reduced cloud fraction in SM\_DEF, time series of rain and cloud water path in regions of shallow convection, defined as all points with PW less than 40 mm, are shown in Fig. 5. The rain and cloud water paths in SM\_DEF both decrease immediately and never recover. The decrease is even larger than that for DM\_A1000—the simulation that was expected to be an approximate limit for the magnitude of cloud property changes. Figure 5 suggests that the large changes in cloud fraction (Fig. 3) and rain rate (Fig. 4) in SM\_DEF are due to fast changes in the microphysics and are not due to a slow adjustment to a new radiative–convective equilibrium state.

The average cloud droplet number concentration in shallow clouds in DM\_A100 is about  $30\text{ cm}^{-3}$  (Fig. 6a), which is much lower than the fixed cloud droplet concentration of  $300\text{ cm}^{-3}$  in SM\_DEF. Given that both

simulations begin with the same cloud water content, cloud droplets in SM\_DEF are immediately made to be about  $1/5$  the size of those in DM\_A100. Conversely, the average raindrop diameter is 0.2–0.5 mm for shallow cumuli (Fig. 6b), which is much lower than the fixed raindrop diameter of 1 mm. These comparisons indicate that cloud droplets are much smaller in SM\_DEF and lead to reduced collision–coalescence and rain production. With less rain, and with much larger raindrops that evaporate more slowly, evaporatively generated cold pools likely diminish in strength and number, thus making new convection more difficult to initiate in SM\_DEF.

### c. Representative parameters

These results suggest that more care should be taken in choosing the fixed parameters in a single-moment scheme. Perhaps the cloud characteristics in SM\_DEF and DM\_A100 would be more similar if the fixed parameter values in SM\_DEF were more representative of the values in DM\_A100. To test this idea, a second single-moment sensitivity simulation was started in the same way as SM\_DEF, but in which the fixed parameter values were taken as the mass-weighted averages of number concentration or diameter of each hydrometeor species from DM\_A100 at the time of the model restart. These values are listed in Table 2 and the simulation is referred to as SM\_AVG. Table 2 shows that some of the parameter values in SM\_DEF, such as aggregate diameter, are in fact quite close to the averages in DM\_A100 that are used for SM\_AVG. However, parameters such as the cloud droplet number concentration and raindrop diameter used in SM\_DEF are not appropriate for representing these microphysical characteristics in DM\_A100.

SM\_AVG developed a low-level downdraft associated with one of the deep convective storms with a speed of  $-18\text{ m s}^{-1}$  after just over 6 h of simulation that was

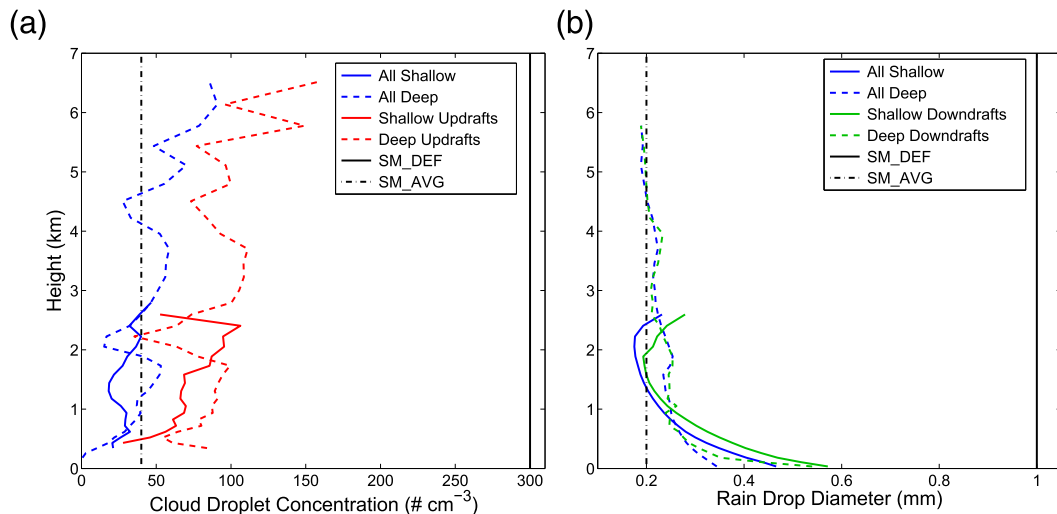


FIG. 6. Colored lines: (a) cloud droplet concentration averaged over cloudy points and (b) mass-weighted raindrop diameter averaged over rainy points in DM\_A100. Cloudy and rainy points defined as having a mixing ratio greater than  $0.01 \text{ g kg}^{-1}$ . Shallow cumulus identified as regions with precipitable water less than 40 mm, deep convection identified as regions with precipitable water greater than 60 mm. Updrafts (downdrafts) defined to be points with vertical velocity greater than  $0.5 \text{ m s}^{-1}$  (less than  $-0.5 \text{ m s}^{-1}$ ). Black lines: fixed values of each parameter in the two single-moment simulations.

incompatible with the vertical grid spacing. Nonetheless, since the largest changes in SM\_DEF occurred in the first 6 h, we can learn from this simulation. The rain-water content in this downdraft was high compared to values found at any time in DM\_A100 (not shown). This suggests that rainwater is being created too quickly in regions of deep convection. While the cloud droplet number concentration is  $40 \text{ cm}^{-3}$  in SM\_AVG, the average cloud droplet number concentration in deep convective updrafts in DM\_A100 is approximately 75–100  $\text{cm}^{-3}$  (Fig. 6a). Assuming that the cloud water contents are similar, this difference in number concentration implies that the cloud droplets in SM\_AVG are too large compared to DM\_A100 in these updrafts and may be causing too-efficient conversion of cloud water to rain. Furthermore, average raindrop sizes increase rapidly in the low-level downdrafts (Fig. 6b) as the smallest drops are evaporated in DM\_A100, though this change in size is counteracted somewhat by the rain breakup process that begins when drops reach 0.6 mm in diameter. These effects are not captured in single-moment simulations. Therefore, the average raindrop size at low levels (where the large downdraft occurred) in SM\_AVG is too small, thus enhancing evaporation and downdraft generation relative to DM\_A100.

Even in the regions of shallow cumulus, SM\_AVG does not appear to have improved the representation of clouds. The cloud water path decreases at about the same rate as in SM\_DEF (Fig. 5a). Rain water in SM\_AVG does not decrease as quickly (Fig. 5b). However, as in the

regions of deep convection, the average raindrop size is too small at low levels compared to DM\_A100 (Fig. 6b) and therefore the rain evaporation process would likely not be well represented. These results suggest that the natural variability in microphysical properties of hydrometeors within all tropical cloud types can be better simulated by double-moment schemes than single-moment schemes.

## 5. Conclusions

Single-moment microphysics schemes run faster but by design predict fewer properties of hydrometeor distributions than double-moment microphysics schemes. It has been shown here through theoretical arguments and simple numerical experiments that the assumptions made in single-moment schemes lead to a large degree of inherent uncertainty in simulations of convective clouds. For example, in a single-moment scheme with a fixed mean cloud droplet diameter, basic microphysical equations indicate that doubling of the diameter can decrease condensation rates by a factor of 4 while increasing autoconversion rates by a factor of 2. Simulations of a deep convective cell using the RAMS single-moment scheme confirm that the microphysical rates are highly sensitive to the choice of parameter to fix and its value. Unlike most other single-moment schemes, RAMS allows the diameter of hydrometeors to be fixed rather than the number concentration or the intercept parameter. The results show that the simulations are

indeed more sensitive to a change in the fixed mean diameter than to the fixed number concentration as predicted by the simple theoretical arguments. This finding may lend support to the choice of a fixed number concentration rather than a fixed mean diameter in single-moment schemes.

The changes in the microphysical rates seen in the idealized thunderstorm simulations feed back to other fields in the simulations. Accumulated precipitation showed up to a 200% increase as a result of observationally based parameter choices in the single-moment scheme. Convective mass flux, surface temperature, short- and longwave radiation, and upper-level moisture are all also sensitive to the fixed parameters of a single-moment scheme. The variability in the radiative fluxes is found to be of similar magnitude to those associated with cloud feedbacks predicted by climate models (Zelinka and Hartmann 2010).

In addition to simulations employing single-moment schemes being sensitive to the choice of parameters and values, they struggle to capture the observed bulk features of tropical clouds such as cloud fraction and rain rate in radiative–convective equilibrium simulations, whereas double-moment schemes, at least the double-moment scheme in RAMS, are more successful with these tasks. Even when every effort is made to choose fixed values in a single-moment scheme that are representative of the system being simulated, our results show that unintended feedbacks can arise owing to the inherently large variability of hydrometeor distribution properties within cloud systems. Similar conclusions have been drawn in studies of squall-line convection, which have found that single-moment schemes cannot simultaneously capture the microphysical properties of the leading line and the trailing stratiform cloud (Morrison et al. 2009; Van Weverberg et al. 2012; Baba and Takahashi 2014). Last, although our RCE simulations are idealized, the results suggest that double-moment schemes better represent tropical clouds than single-moment schemes when compared with observations.

The focus in this study has been primarily on the warm phase. To confirm further that double-moment schemes outperform single-moment schemes, more detailed analysis of the ice phase should be done in a future study. In addition, though not explored in this study, it is recognized that single-moment schemes with parameters diagnosed from environmental conditions may mitigate some of the issues with more traditional single-moment schemes (Roh and Satoh 2014), such as the one used in this study. Last, as discussed in the introduction, while double-moment schemes eliminate some of the assumptions required in single-moment schemes, they do

introduce new assumptions that in some cases do not result in any improvement to simulations (e.g., Van Weverberg et al. 2014). Nonetheless, it seems that double-moment schemes should be able to represent simultaneously better the characteristics of multiple cloud types in a single simulation even if a single-moment scheme can predict the characteristics of any one cloud type as well or better.

It is acknowledged that the use of single-moment schemes may sometimes be desirable in order to understand specific feedback processes, to constrain intentionally the model for various experiments, in simple model frameworks in which the equations are oversimplified intentionally for specific purposes or in very-long-time simulations such as those used for climate predictions. However, if one of those situations is not the case, it is argued based on our results and those of others (Reisner et al. 1998; Swann 1998; Luo et al. 2008; Morrison et al. 2009; Dawson et al. 2010; Milbrandt et al. 2010; Lee and Donner 2011; Jung et al. 2012; Molthan and Colle 2012; Van Weverberg et al. 2012; Baba and Takahashi 2014; Jin et al. 2014) that the improvement in the representation of clouds and cloud feedbacks gained by use of a double-moment scheme (or other added complexity schemes such as triple-moment or spectral bin schemes) is well worth the extra expense in computational time and should be strongly considered in all but the lengthiest simulations where realistic reproduction of the atmosphere is desired.

*Acknowledgments.* The authors thank Emily Parker for her assistance in the analysis of the thunderstorm simulations and acknowledge the support given to her by the Center for Multiscale Modeling of Atmospheric Processes Undergraduate Research Opportunities program. The authors also thank the three anonymous reviewers for their constructive comments that led to improvements to this paper. This material is based upon work supported by the National Science Foundation Graduate Research Fellowship Program under Grant DGE-1321845. This work was also supported by NASA Headquarters under the NASA Earth and Space Science Fellowship Program Grant NNX 13AN66H and NASA Grant NNX 13AQ33G.

## APPENDIX

### Justification of Model Restart

It could be argued that the method of restarting a simulation with a different microphysics scheme as was done here is too strong a “shock” to the model and that differences between the original and restarted simulations

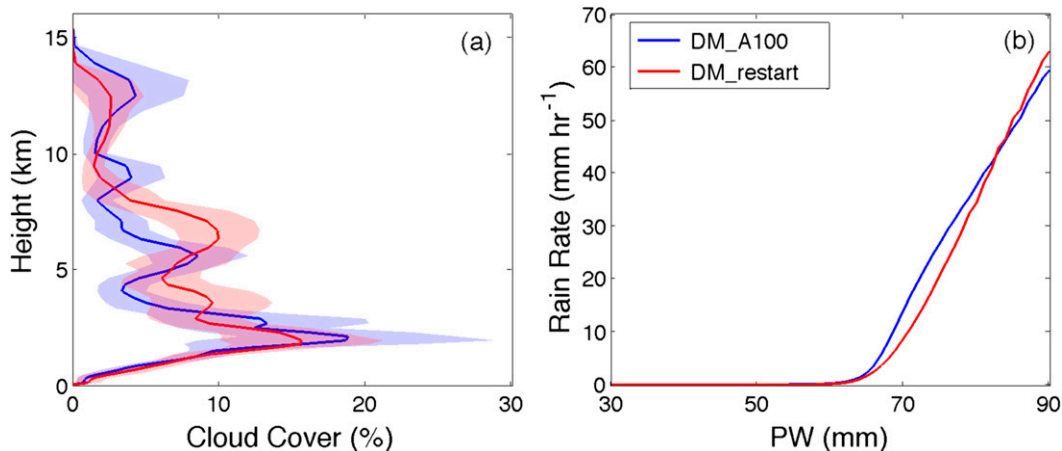


FIG. A1. As in (a) Fig. 3 and (b) Fig. 4, but for DM\_A100 and DM\_restart. The values for DM\_restart are averaged over the first 48 h of the simulation.

are a result of this shock. To test if this is the case, SM\_DEF is restarted from its fifth simulation hour with the double-moment scheme turned back on (DM\_restart) and run for 5 days. Such a restart does not produce a shock to the model because the initial hydrometeor mixing ratios and number concentrations are identical to those in SM\_DEF. If the shock is the primary cause of the rapid changes, then DM\_restart, which has no shock, should continue to behave like SM\_DEF. If the shock is not the primary cause of the rapid changes in cloud properties, then DM\_restart should also rapidly return to a state similar to DM\_A100.

Rapid changes to the cloud and rain properties are in fact seen in DM\_restart. The cloud fraction and rain rate values become similar to those seen in Figs. 3 and 4 within 2 days (Fig. A1) with the most rapid increases occurring within the first 10 h of the simulation. [Over the next 3 days, the low-cloud fraction increases beyond the average seen in Fig. A1a and then decreases again (not shown). While the average over this 3-day period is higher than that seen in Fig. A1a, it is believed that the simulation would eventually return to the average value. Such large fluctuations are not seen in SM\_DEF and thus are not of concern for the validity of the results arising from that simulation.] This result strongly suggests these RCE simulations respond very quickly to changes to the microphysics scheme. Furthermore, the cloud fraction in SM\_DEF is very similar to the cloud fraction presented by Posselt et al. (2008) as part of a similar RCE modeling study utilizing a single-moment scheme (their Fig. 2b). While the responses seen in SM\_DEF within the first hour are likely a result of the model shock, it is unlikely that the long-term responses are also a result of the model shock. Rather, they are physical changes

that could be expected to persist if the model were run for additional days or if the simulation had been started at time zero.

#### REFERENCES

- Adams-Selin, R. D., S. C. van den Heever, and R. H. Johnson, 2013: Impact of graupel parameterization schemes on idealized bow echo simulations. *Mon. Wea. Rev.*, **141**, 1241–1262, doi:10.1175/MWR-D-12-00064.1.
- Baba, Y., and K. Takahashi, 2014: Dependency of stratiform precipitation on a two-moment cloud microphysical scheme in mid-latitude squall line. *Atmos. Res.*, **138**, 394–413, doi:10.1016/j.atmosres.2013.12.009.
- Baker, M. B., 1993: Variability in concentrations of cloud condensation nuclei in the marine cloud-topped boundary layer. *Tellus*, **45B**, 458–472, doi:10.1034/j.1600-0889.45.issue5.1.x.
- Boucher, O., H. Le Treut, and M. B. Baker, 1995: Precipitation and radiation modeling in a general circulation model: Introduction of cloud microphysical processes. *J. Geophys. Res.*, **100**, 16 395–16 414, doi:10.1029/95JD01382.
- Connolly, P. J., A. J. Heymsfield, and T. W. Choullarton, 2006: Modelling the influence of rimer surface temperature on the glaciation of intense thunderstorms: The rime-splinter mechanism of ice multiplication. *Quart. J. Roy. Meteor. Soc.*, **132**, 3059–3077, doi:10.1256/qj.05.45.
- Cotton, W. R., and Coauthors, 2003: RAMS 2001: Current status and future directions. *Meteor. Atmos. Phys.*, **82**, 5–29, doi:10.1007/s00703-001-0584-9.
- Dawson, D. T., M. Xue, J. A. Milbrandt, and M. K. Yau, 2010: Comparison of evaporation and cold pool development between single-moment and multimoment bulk microphysics schemes in idealized simulations of tornadic thunderstorms. *Mon. Wea. Rev.*, **138**, 1152–1171, doi:10.1175/2009MWR2956.1.
- Feingold, G., R. L. Walko, B. Stevens, and W. R. Cotton, 1998: Simulations of marine stratocumulus using a new microphysical parameterization scheme. *Atmos. Res.*, **47–48**, 505–528, doi:10.1016/S0169-8095(98)00058-1.
- Ferrier, B., 1994: A double-moment multiple-phase four-class bulk ice scheme. Part I: Description. *J. Atmos. Sci.*, **51**, 249–280, doi:10.1175/1520-0469(1994)051<0249:ADMMPF>2.0.CO;2.

- , W.-K. Tao, and J. Simpson, 1995: A double-moment multiple-phase four-class bulk ice scheme. Part II: Simulations of convective storms in different large-scale environments and comparisons with other bulk parameterizations. *J. Atmos. Sci.*, **52**, 1001–1033, doi:10.1175/1520-0469(1995)052<1001:ADMMPF>2.0.CO;2.
- Gilmore, M. S., E. N. Rasmussen, and J. M. Straka, 2004: Precipitation uncertainty due to variations in precipitation particle parameters within a simple microphysics scheme. *Mon. Wea. Rev.*, **132**, 2610–2627, doi:10.1175/MWR2810.1.
- Harrington, J. Y., 1997: The effects of radiative and microphysical processes on simulation warm and transition season Arctic stratus. Ph.D. dissertation, Colorado State University, 289 pp. [Available from Department of Atmospheric Science, Colorado State University, 3915 West Laport Avenue, Fort Collins, CO 80523.]
- Hong, S.-Y., and J.-O. J. Lim, 2006: The WRF single-moment 6-class microphysics scheme (WSM6). *J. Korean Meteor. Soc.*, **42**, 129–151.
- , J. Dudhia, and S.-H. Chen, 2004: A revised approach to ice microphysical processes for the bulk parameterization of clouds and precipitation. *Mon. Wea. Rev.*, **132**, 103–120, doi:10.1175/1520-0493(2004)132<0103:ARATIM>2.0.CO;2.
- , K.-S. S. Lim, Y.-H. Lee, J.-C. Ha, H.-W. Kim, S.-J. Ham, and J. Dudhia, 2010: Evaluation of the WRF Double-Moment 6-Class Microphysics scheme for precipitating convection. *Adv. Meteor.*, **2010**, 707253, doi:10.1155/2010/707253.
- Jin, Y., and Coauthors, 2014: The impact of ice phase cloud parameterizations on tropical cyclone prediction. *Mon. Wea. Rev.*, **142**, 606–625, doi:10.1175/MWR-D-13-00058.1.
- Johnson, R. H., T. M. Rickenbach, S. A. Rutledge, P. E. Ciesielski, and W. H. Schubert, 1999: Trimodal characteristics of tropical convection. *J. Climate*, **12**, 2397–2418, doi:10.1175/1520-0442(1999)012<2397:TCOTC>2.0.CO;2.
- Jung, Y., M. Xue, and M. Tong, 2012: Ensemble Kalman filter analyses of the 29–30 May 2004 Oklahoma tornadic thunderstorm using one- and two-moment bulk microphysics schemes, with verification against polarimetric radar data. *Mon. Wea. Rev.*, **140**, 1457–1475, doi:10.1175/MWR-D-11-00032.1.
- Khain, A., A. Pokrovsky, M. Pinsky, A. Seifert, and V. Phillips, 2004: Simulation of effects of atmospheric aerosols on deep turbulent convective clouds using a spectral microphysics mixed-phase cumulus cloud model. Part I: Model description and possible applications. *J. Atmos. Sci.*, **61**, 2963–2982, doi:10.1175/JAS-3350.1.
- Lebo, Z. J., and J. H. Seinfeld, 2011: Theoretical basis for convective invigoration due to increased aerosol concentration. *Atmos. Chem. Phys.*, **11**, 5407–5429, doi:10.5194/acp-11-5407-2011.
- , H. Morrison, and J. H. Seinfeld, 2012: Are simulated aerosol-induced effects on deep convective clouds strongly dependent on saturation adjustment? *Atmos. Chem. Phys.*, **12**, 9941–9964, doi:10.5194/acp-12-9941-2012.
- Lee, S. S., and L. J. Donner, 2011: Effects of cloud parameterization on radiation and precipitation: A comparison between single-moment microphysics and double-moment microphysics. *Terr. Atmos. Ocean. Sci.*, **22**, 403, doi:10.3319/TAO.2011.03.03.01(A).
- Lin, Y.-L., R. D. Farley, and H. D. Orville, 1983: Bulk parameterization of the snow field in a cloud model. *J. Climate Appl. Meteor.*, **22**, 1065–1092, doi:10.1175/1520-0450(1983)022<1065:BPOTSF>2.0.CO;2.
- Liu, Y., and P. H. Daum, 2004: Parameterization of the autoconversion process. Part I: Analytical formulation of the Kessler-type parameterizations. *J. Atmos. Sci.*, **61**, 1539–1548, doi:10.1175/1520-0469(2004)061<1539:POTAPI>2.0.CO;2.
- Luo, Y., K.-M. Xu, H. Morrison, and G. McFarquhar, 2008: Arctic mixed-phase clouds simulated by a cloud-resolving model: Comparison with ARM observations and sensitivity to microphysics parameterizations. *J. Atmos. Sci.*, **65**, 1285–1303, doi:10.1175/2007JAS2467.1.
- Mace, G. G., Q. Zhang, M. Vaughan, R. Marchand, G. Stephens, C. Trepte, and D. Winker, 2009: A description of hydrometeor layer occurrence statistics derived from the first year of merged Cloudsat and CALIPSO data. *J. Geophys. Res.*, **114**, D00A26, doi:10.1029/2007JD009755.
- Mansell, E. R., 2010: On sedimentation and advection in multi-moment bulk microphysics. *J. Atmos. Sci.*, **67**, 3084–3094, doi:10.1175/2010JAS3341.1.
- , C. L. Ziegler, and E. C. Bruning, 2010: Simulated electrification of a small thunderstorm with two-moment bulk microphysics. *J. Atmos. Sci.*, **67**, 171–194, doi:10.1175/2009JAS2965.1.
- Manton, M., and W. Cotton, 1977: Formulation of approximate equations for modeling moist deep convection on the meso-scale. Colorado State University Atmospheric Science Paper 266, 62 pp.
- Medeiros, B., L. Nuijens, C. Antoniazzi, and B. Stevens, 2010: Low-latitude boundary layer clouds as seen by CALIPSO. *J. Geophys. Res.*, **115**, D23207, doi:10.1029/2010JD014437.
- Meyers, M. P., R. L. Walko, J. Y. Harrington, and W. R. Cotton, 1997: New RAMS cloud microphysics parameterization. Part II: The two-moment scheme. *Atmos. Res.*, **45**, 3–39, doi:10.1016/S0169-8095(97)00018-5.
- Milbrandt, J. A., and M. K. Yau, 2005a: A multimoment bulk microphysics parameterization. Part I: Analysis of the role of the spectral shape parameter. *J. Atmos. Sci.*, **62**, 3051–3064, doi:10.1175/JAS3534.1.
- , and —, 2005b: A multimoment bulk microphysics parameterization. Part II: A proposed three-moment closure and scheme description. *J. Atmos. Sci.*, **62**, 3065–3081, doi:10.1175/JAS3535.1.
- , and R. McTaggart-Cowan, 2010: Sedimentation-induced errors in bulk microphysics schemes. *J. Atmos. Sci.*, **67**, 3931–3948, doi:10.1175/2010JAS3541.1.
- , M. K. Yau, J. Mailhot, S. Bélair, and R. McTaggart-Cowan, 2010: Simulation of an orographic precipitation event during IMPROVE-2. Part II: Sensitivity to the number of moments in the bulk microphysics scheme. *Mon. Wea. Rev.*, **138**, 625–642, doi:10.1175/2009MWR3121.1.
- Molthan, A. L., and B. A. Colle, 2012: Comparisons of single- and double-moment microphysics schemes in the simulation of a synoptic-scale snowfall event. *Mon. Wea. Rev.*, **140**, 2982–3002, doi:10.1175/MWR-D-11-00292.1.
- Morrison, H., and J. Milbrandt, 2011: Comparison of two-moment bulk microphysics schemes in idealized supercell thunderstorm simulations. *Mon. Wea. Rev.*, **139**, 1103–1130, doi:10.1175/2010MWR3433.1.
- , J. A. Curry, and V. I. Khvorostyanov, 2005: A new double-moment microphysics parameterization for application in cloud and climate models. Part I: Description. *J. Atmos. Sci.*, **62**, 1665–1677, doi:10.1175/JAS3446.1.
- , G. Thompson, and V. Tatarskii, 2009: Impact of cloud microphysics on the development of trailing stratiform precipitation in

- a simulated squall line: Comparison of one- and two-moment schemes. *Mon. Wea. Rev.*, **137**, 991–1007, doi:10.1175/2008MWR2556.1.
- , S. A. Tessoro, K. Ikeda, and G. Thompson, 2012: Sensitivity of a simulated midlatitude squall line to parameterization of raindrop breakup. *Mon. Wea. Rev.*, **140**, 2437–2460, doi:10.1175/MWR-D-11-00283.1.
- Neelin, J. D., O. Peters, and K. Hales, 2009: The transition to strong convection. *J. Atmos. Sci.*, **66**, 2367–2384, doi:10.1175/2009JAS2962.1.
- Onishi, R., and K. Takahashi, 2012: A warm-bin–cold-bulk hybrid cloud microphysical model. *J. Atmos. Sci.*, **69**, 1474–1497, doi:10.1175/JAS-D-11-0166.1.
- Ovtchinnikov, M., and Y. L. Kogan, 2000: An investigation of ice production mechanisms in small cumuliform clouds using a 3D model with explicit microphysics. Part I: Model description. *J. Atmos. Sci.*, **57**, 2989–3003, doi:10.1175/1520-0469(2000)057<2989:AIOIPM>2.0.CO;2.
- Posselt, D. J., S. C. van den Heever, and G. L. Stephens, 2008: Trimodal cloudiness and tropical stable layers in simulations of radiative convective equilibrium. *Geophys. Res. Lett.*, **35**, L08802, doi:10.1029/2007GL033029.
- Pruppacher, H. R., and J. D. Klett, 2010: *Microphysics of Clouds and Precipitation*. 2nd ed. Atmospheric and Oceanographic Sciences Library, Vol. 18, Springer, 976 pp.
- Rasmussen, R. M., I. Geresdi, G. Thompson, K. Manning, and E. Karplus, 2002: Freezing drizzle formation in stably stratified layer clouds: The role of radiative cooling of cloud droplets, cloud condensation nuclei, and ice initiation. *J. Atmos. Sci.*, **59**, 837–860, doi:10.1175/1520-0469(2002)059<0837:FDFISS>2.0.CO;2.
- Reisin, T., Z. Levin, and S. Tzivion, 1996: Rain production in convective clouds as simulated in an axisymmetric model with detailed microphysics. Part I: Description of the model. *J. Atmos. Sci.*, **53**, 497–519, doi:10.1175/1520-0469(1996)053<0497:RPICCA>2.0.CO;2.
- Reisner, J., R. M. Rasmussen, and R. T. Bruintjes, 1998: Explicit forecasting of supercooled liquid water in winter storms using the MM5 mesoscale model. *Quart. J. Roy. Meteor. Soc.*, **124**, 1071–1107, doi:10.1002/qj.49712454804.
- Roh, W., and M. Satoh, 2014: Evaluation of precipitating hydrometeor parameterizations in a single-moment bulk microphysics scheme for deep convective systems over the tropical central Pacific. *J. Atmos. Sci.*, **71**, 2654–2673, doi:10.1175/JAS-D-13-0252.1.
- Saleeby, S. M., and W. R. Cotton, 2004: A large-droplet mode and prognostic number concentration of cloud droplets in the Colorado State University Regional Atmospheric Modeling System (RAMS). Part I: Module descriptions and supercell test simulations. *J. Appl. Meteor.*, **43**, 182–195, doi:10.1175/1520-0450(2004)043<0182:ALMAPN>2.0.CO;2.
- , and —, 2008: A binned approach to cloud-droplet riming implemented in a bulk microphysics model. *J. Appl. Meteor. Climatol.*, **47**, 694–703, doi:10.1175/2007JAMC1664.1.
- , and S. C. van den Heever, 2013: Developments in the CSU-RAMS aerosol model: Emissions, nucleation, regeneration, deposition, and radiation. *J. Appl. Meteor. Climatol.*, **52**, 2601–2622, doi:10.1175/JAMC-D-12-0312.1.
- Seifert, A., and K. D. Beheng, 2006: A two-moment cloud microphysics parameterization for mixed-phase clouds. Part I: Model description. *Meteor. Atmos. Phys.*, **92**, 45–66, doi:10.1007/s00703-005-0112-4.
- Shima, S., K. Kusano, A. Kawano, T. Sugiyama, and S. Kawahara, 2009: The super-droplet method for the numerical simulation of clouds and precipitation: A particle-based and probabilistic microphysics model coupled with a non-hydrostatic model. *Quart. J. Roy. Meteor. Soc.*, **135**, 1307–1320, doi:10.1002/qj.441.
- Smagorinsky, J., 1963: General circulation experiments with the primitive equations. *Mon. Wea. Rev.*, **91**, 99–164, doi:10.1175/1520-0493(1963)091<0099:GCEWTP>2.3.CO;2.
- Straka, J., and E. Mansell, 2005: A bulk microphysics parameterization with multiple ice precipitation categories. *J. Appl. Meteor.*, **44**, 445–466, doi:10.1175/JAM2211.1.
- Swann, H., 1998: Sensitivity to the representation of precipitating ice in CRM simulations of deep convection. *Atmos. Res.*, **47–48**, 415–435, doi:10.1016/S0169-8095(98)00050-7.
- Thompson, D. W. J., and Coauthors, 2012: The mystery of recent stratospheric temperature trends. *Nature*, **491**, 692–697, doi:10.1038/nature11579.
- Thompson, G., R. M. Rasmussen, and K. Manning, 2004: Explicit forecasts of winter precipitation using an improved bulk microphysics scheme. Part I: Description and sensitivity analysis. *Mon. Wea. Rev.*, **132**, 519–542, doi:10.1175/1520-0493(2004)132<0519:EFOWPU>2.0.CO;2.
- , P. R. Field, W. D. Hall, and R. M. Rasmussen, 2008: Explicit forecasts of winter precipitation using an improved bulk microphysics scheme. Part II: Implementation of a new snow parameterization. *Mon. Wea. Rev.*, **136**, 5095–5115, doi:10.1175/2008MWR2387.1.
- Tompkins, A. M., 2001: Organization of tropical convection in low vertical wind shears: The role of cold pools. *J. Atmos. Sci.*, **58**, 1650–1672, doi:10.1175/1520-0469(2001)058<1650:OOTCIL>2.0.CO;2.
- van den Heever, S. C., and W. R. Cotton, 2004: The impact of hail size on simulated supercell storms. *J. Atmos. Sci.*, **61**, 1596–1609, doi:10.1175/1520-0469(2004)061<1596:TIOHSO>2.0.CO;2.
- , G. L. Stephens, and N. B. Wood, 2011: Aerosol indirect effects on tropical convection characteristics under conditions of radiative–convective equilibrium. *J. Atmos. Sci.*, **68**, 699–718, doi:10.1175/2010JAS3603.1.
- Van Weverberg, K., A. M. Vogelmann, H. Morrison, and J. A. Milbrandt, 2012: Sensitivity of idealized squall-line simulations to the level of complexity used in two-moment bulk microphysics schemes. *Mon. Wea. Rev.*, **140**, 1883–1907, doi:10.1175/MWR-D-11-00120.1.
- , and Coauthors, 2013: The role of cloud microphysics parameterization in the simulation of mesoscale convective system clouds and precipitation in the tropical western Pacific. *J. Atmos. Sci.*, **70**, 1104–1128, doi:10.1175/JAS-D-12-0104.1.
- , E. Goudenhoofd, U. Blahak, E. Brisson, M. Demuzere, P. Marbaix, and J.-P. van Ypersele, 2014: Comparison of one-moment and two-moment bulk microphysics for high-resolution climate simulations of intense precipitation. *Atmos. Res.*, **147–148**, 145–161, doi:10.1016/j.atmosres.2014.05.012.
- Wacker, U., and A. Seifert, 2001: Evolution of rain water profiles resulting from pure sedimentation: Spectral vs. parameterized description. *Atmos. Res.*, **58**, 19–39, doi:10.1016/S0169-8095(01)00081-3.
- , and C. Lüpkes, 2009: On the selection of prognostic moments in parameterization schemes for drop sedimentation. *Tellus*, **61A**, 498–511, doi:10.1111/j.1600-0870.2009.00405.x.
- Walko, R. L., W. R. Cotton, M. P. Meyers, and J. Y. Harrington, 1995: New RAMS cloud microphysics parameterization part I: The single-moment scheme. *Atmos. Res.*, **38**, 29–62, doi:10.1016/0169-8095(94)00087-T.



- Weisman, M., and J. Klemp, 1982: The dependence of numerically simulated convective storms on vertical wind shear and buoyancy. *Mon. Wea. Rev.*, **110**, 504–520, doi:[10.1175/1520-0493\(1982\)110<0504:TDONSC>2.0.CO;2](https://doi.org/10.1175/1520-0493(1982)110<0504:TDONSC>2.0.CO;2).
- Wu, L., and G. W. Petty, 2010: Intercomparison of bulk microphysics schemes in model simulations of polar lows. *Mon. Wea. Rev.*, **138**, 2211–2228, doi:[10.1175/2010MWR3122.1](https://doi.org/10.1175/2010MWR3122.1).
- Yussouf, N., and D. J. Stensrud, 2012: Comparison of single-parameter and multiparameter ensembles for assimilation of radar observations using the ensemble Kalman filter. *Mon. Wea. Rev.*, **140**, 562–586, doi:[10.1175/MWR-D-10-05074.1](https://doi.org/10.1175/MWR-D-10-05074.1).
- Zelinka, M. D., and D. L. Hartmann, 2010: Why is longwave cloud feedback positive? *J. Geophys. Res.*, **115**, D16117, doi:[10.1029/2010JD013817](https://doi.org/10.1029/2010JD013817).